Cooperativity and anti-cooperativity between ligand binding and the dimerization of ristocetin A: asymmetry of a homodimer complex and implications for signal transduction

Younghoon R Cho, Alison J Maguire, Andrew C Try, Martin S Westwell, Patrick Groves† and Dudley H Williams*

Background: Recent work has indicated that dimerization is important in the mode of action of the vancomycin group of glycopeptide antibiotics. NMR studies have shown that one member of this group, ristocetin A, forms an asymmetric dimer with two physically different binding sites for cell wall peptides. Ligand binding by ristocetin A and dimerization are slightly anti-cooperative. In contrast, for the other glycopeptide antibiotics of the vancomycin group that have been examined so far, binding of cell wall peptides and dimerization are cooperative.

Results: Here we show that the two halves of the asymmetric homodimer formed by ristocetin A have different affinities for ligand binding. One of these sites is preferentially filled before the other, and binding to this site is cooperative with dimerization. Ligand binding to the other, less favored half of the dimer, is anti-cooperative with dimerization.

Conclusions: In dimer complexes, anti-cooperativity of dimerization upon ligand binding can be a result of asymmetry, in which two binding sites have different affinities for ligands. Such a system, in which one binding site is filled preferentially, may be a mechanism by which the cooperativity between ligand binding and dimerization is fine tuned and may thus have relevance to the control of signal transduction in biological systems.

Address: Cambridge Centre for Molecular Recognition, University Chemical Laboratories, University of Cambridge, Lensfield Road, Cambridge, CB2 1EW, UK.

†Present address: Physical Chemistry 2, University of Lund, Box 124, 22100 Lund, Sweden.

*Corresponding author.

Key words: anti-cooperativity, asymmetry, dimerization, ristocetin A

Received: **26 Feb 1996**
Accepted: **13 Mar 1996**

Chemistry & Biology March 1996, **3**:207–215

 ISSN 1074-5521

Introduction

The vancomycin group of glycopeptide antibiotics have a heptapeptide backbone with many common residues. The backbone is oxidatively cross-linked through aromatic side chains, and may carry sugar substituents of various types [1,2], as illustrated for ristocetin A in Figure 1. The molecular basis for their antibacterial action has been extensively studied and arises from specific binding of the antibiotic to nascent bacterial cell-wall peptides terminating in -D-Ala-D-Ala [3,4]. The proposed hydrogen-bonding scheme between the cell-wall analogue *N*-acetyl-D-Ala-D-Ala (*N*-ac-DADA) and ristocetin A is shown in Figure 1 [5]. Furthermore, dimerization of these glycopeptide antibiotics has been implicated in their mode of action [6–8].

Recent NMR studies have revealed that both ristocetin A (Fig. 2a) and eremomycin form asymmetric homodimers [5,9]. The glycopeptides A82846B [10] and ureido-balhimycin [11] also form such structures (as shown by NMR and X-ray crystallography, respectively). In all cases, the asymmetry arises because the head-to-tail arrangement of the peptide backbones in the dimer, which have two-fold (C_2) rotational symmetry, contrasts with the head-to-head arrangement of the sugar substituent on residue 4 of the antibiotics (a tetrasaccharide for ristocetin A, Fig. 2b). The parallel orientation of the tetrasaccharides results in two distinct binding sites; one site is capped by the rhamnose of the tetrasaccharide, and the other by the arabinose [5]. NMR titration studies with di-*N*-acetyl-L-Lys-D-Ala-D-Ala (di-*N*-ac-KDADA) established that the site capped by the rhamnose sugar (designated D_1) has a higher affinity for cell-wall analogues and binds ligand in preference to the site capped by the arabinose sugar (designated D_2) [5,7]. The difference in ligand binding affinities between the two sites was also shown using ^{13}C-labelled *N*-ac-DADA [12].

Cooperativity between ligand binding and dimerization has previously been observed for all members of the vancomycin family that dimerize, apart from ristocetin A. The binding of one equivalent of the ligand di-*N*-ac-KDADA to ristocetin A has the net effect of slightly decreasing the dimerization constant [13]. Ristocetin pseudo-agylcone (ristocetin-Ψ), which lacks the tetrasaccharide and the mannose attached to the residue 7 sidechain, displays positive cooperativity between dimerization and ligand binding, suggesting that the origin of anti-cooperativity for ristocetin A may lie in the saccharides [7].

Figure 1

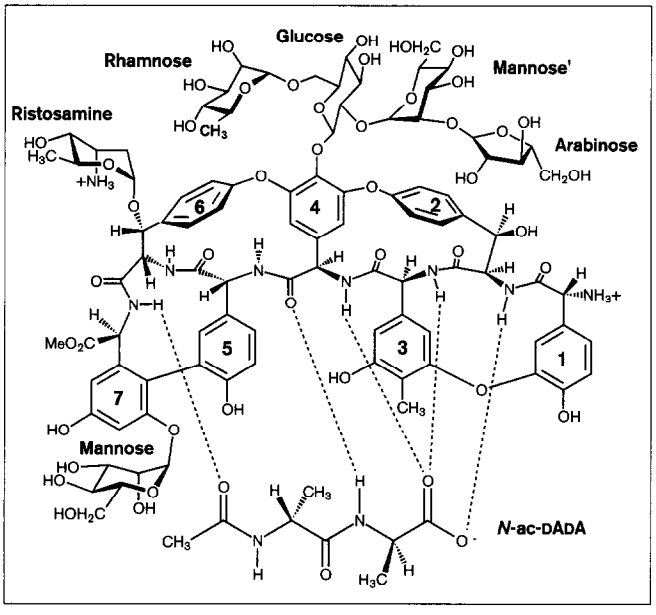

Exploded view of the ristocetin A complex with the cell-wall analogue *N*-ac-DADA. Hydrogen bonds are indicated by dotted lines. The aromatic side chains are numbered from the amino terminus.

Here, we take a quantitative approach to analyze the different binding affinities of the two ligand-binding sites in the ristocetin A dimer and the anti-cooperative relationship between ligand binding and dimerization, and discuss the possible relevance of cooperativity to biological systems such as signal transduction.

Results and discussion

To gain further insight into the anti-cooperativity of formation of the ristocetin A dimer we have used two spectroscopic probes. The first of these is the rhamnose methyl group (Rh_6 methyl) of the tetrasaccharide on the residue 4 sidechain of the antibiotic. Due to the asymmetry of the dimer, the Rh_6 methyl resonances appear as two distinct signals in the NMR spectrum. In addition, an Rh_6 methyl signal from the ristocetin A monomer is observed between the two dimer resonances. Each of these signals are shifted upon complexation with ligand. As the two forms of ristocetin A (monomer/dimer) are in slow exchange on the NMR timescale, their relative populations can be measured as the cell-wall peptide analogue is titrated into a solution of the antibiotic. The effect of added ligand upon dimerization can thus be monitored. The second probe used was the carboxy-terminal D-alanine methyl group of di-*N*-ac-KDADA. This methyl group undergoes a characteristic upfield chemical shift on binding to the glycopeptide antibiotics, from 1.4 ppm (for the free ligand) to around 0.6 ppm (bound ligand) [7]. The ligand bound to ristocetin A appears as two distinct signals corresponding to the two binding sites of the dimer. A ligand-bound monomer signal is also observed and overlaps with the signal of the ligand bound to the less favored dimer site [7]. The use of this probe yields a more quantitative comparison of the different binding affinities of the two binding sites in the dimer.

The first binding event is cooperative, the second anti-cooperative

Changes in the relative populations of monomeric and dimeric ristocetin A were monitored during the stepwise addition of up to one molar equivalent of *N*-ac-DADA. Selected spectra are illustrated in Figure 3. In the

Figure 2

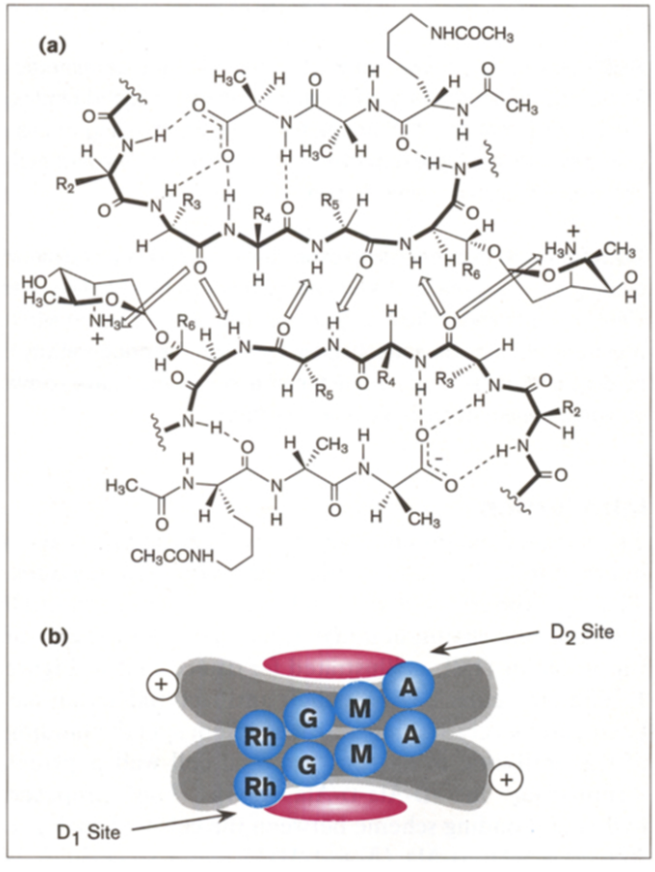

The ristocetin A dimer is asymmetric. **(a)** The hydrogen-bonding network of the peptide backbone at the ristocetin A dimer interface when bound to di-*N*-ac-KDADA. The carboxyl-terminus of the peptide backbone on one half of the dimer interacts with the amino-terminus of the other half. The arrows represent hydrogen bonds formed between the two antibiotic molecules and the dashed lines indicate hydrogen bonds between ristocetin A and di-*N*-ac-KDADA. **(b)** Schematic diagram illustrating the physical basis for the asymmetry of the ristocetin A dimer based on 2D NMR [5]. The peptide backbones of the dimer structure are in an anti-parallel arrangement, in contrast with the parallel arrangement of the tetrasaccharides (Rh = rhamnose, G = glucose, M = mannose, A = arabinose). The rhamnose sugar 'caps' the ligand in the one site, whereas the arabinose of the other tetrasaccharide has a similar role in the second site.

absence of ligand, the ^{1}H NMR resonance of the Rh_6 methyl group of the monomer appears at 1.08 ppm (Fig. 3a), whereas in the dimeric form, two signals of equal intensity are observed at 0.89 ppm and 1.29 ppm, with a relative abundance of monomer and dimer species of ~1:1. During the first half of the titration (Fig. 3b), ligand binding induces the formation of more dimer, relative to monomer; however, during the second half of the titration (Fig. 3c), ligand binding to the D_2 site results in a reduction in the population of dimer. Thus, although the first binding event is cooperative with dimer formation, the second binding event is anti-cooperative with dimerization.

The D1 site of the dimer is higher affinity than D2

To determine the relative ligand binding affinities of the two sites in the dimer, we used the carboxy-terminal D-alanine methyl group of di-*N*-ac-KDADA as a probe. The titration was effectively performed in the absence of monomer by using a high concentration of antibiotic (50 mM). The cell-wall peptide analogue di-*N*-ac-KDADA was used in place of *N*-ac-DADA as it binds ~10-fold more tightly to the antibiotic [14]. The addition of very small amounts of ligand to the concentrated antibiotic solution ensured that there were only negligible amounts of the doubly bound dimer species present at the beginning of the titration. The experiment was conducted at a lower temperature (283 K) to reduce the rate of exchange between each of the species, such that they are in slow (rather than intermediate) exchange.

After the first addition of ligand (0.06 eq. di-*N*-ac-KDADA, Fig. 4b), it was possible to determine the relative populations of the ligand bound into the favored binding site, denoted $\underline{L}$:D_1D_2 (ligand bound to the D_1 site of the dimer when the D_2 site is free), and the less favored binding site, denoted D_1D_2:$\underline{L}$ (ligand bound to the D_2 site of the dimer when the D_1 site is free). The integration of the carboxy-terminal D-alanine methyl group of the $\underline{L}$:D_1D_2 and D_1D_2:$\underline{L}$ complexes at 0.06 equivalents of di-*N*-ac-KDADA shows that the $\underline{L}$:D_1D_2 population is greater than that of D_1D_2:$\underline{L}$ by a factor of 8 ± 2.0. This represents a free energy difference of ~4.9 ± 0.5 kJ mol^{-1} between the two binding sites.

After addition of 0.23 equivalents of ligand (Fig. 4d), the signal representing the doubly bound species, denoted L:D_1D_2:$\underline{L}$ (resonance from the ligand bound to the D_2 site of the dimer when the D_1 site is also bound), is present. As more ligand is added, the doubly bound dimer species, denoted by L:D_1D_2:L, gradually becomes the dominant species. At 1.0 eq. of di-*N*-ac-KDADA (50 mM), the ligand signals $\underline{L}$:D_1D_2:L (resonance from the ligand bound to the D_1 site of the dimer when the D_2 site is also bound) and L:D_1D_2:$\underline{L}$ are seen as doublets at 0.59 and 0.51 ppm respectively (Fig. 4l).

Figure 3

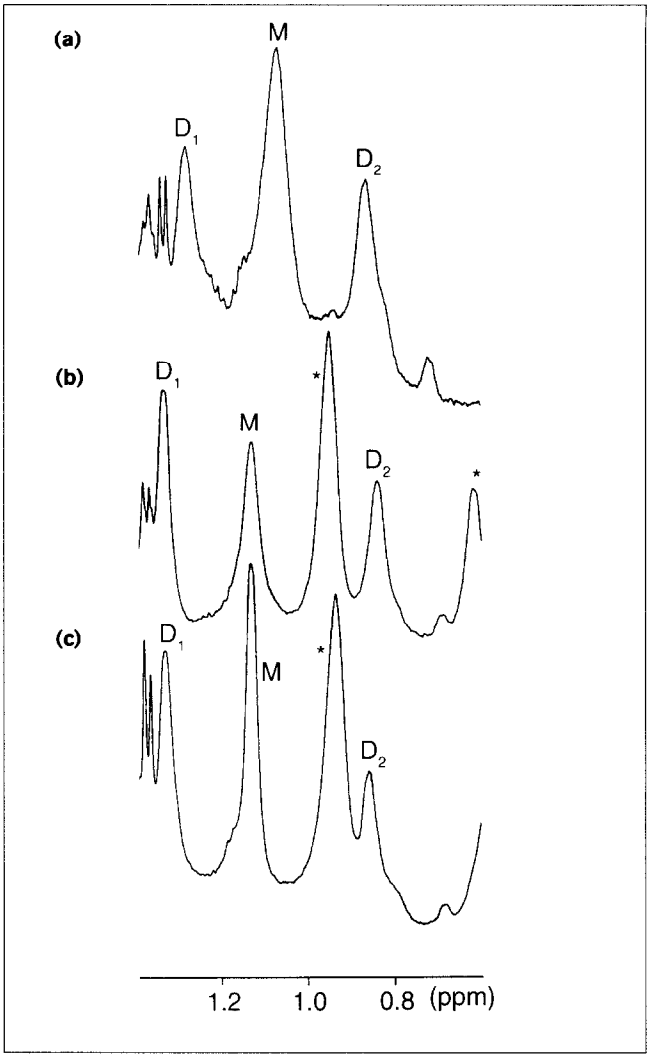

Binding of ligand to the first site in the ristocetin A dimer is cooperative with dimerization, whereas binding to the second site is anti-cooperative. The spectra shown are 500 MHz ^{1}H NMR spectra (D_2O) at 295 K of the Rh_6 methyl signals of **(a)** ristocetin A alone (3 mM), or ristocetin A in the presence of **(b)** 0.5 equivalents or **(c)** 1.0 equivalent of *N*-ac-DADA. The peaks labelled with an asterisk are due to the two alanine methyl groups in the ligand. M refers to the resonance of the Rh_6 methyl group in the monomer; D_1 and D_2 refer to the two resonances observed for the Rh_6 methyl groups in the dimer.

From these spectra, we could assign each of the bound carboxy-terminal D-alanine methyl resonances that arise during various stages of the titration and determine the relative ligand binding affinities of each half of the dimer. The spectra indicate that the D1 site of the ristocetin A dimer has much higher affinity for ligand than the D2 site.

The D1 binding site of the dimer has higher affinity than that of the monomer

To examine the relative affinities of the different binding sites on the dimer and the monomer, the cell-wall analogue

Figure 4

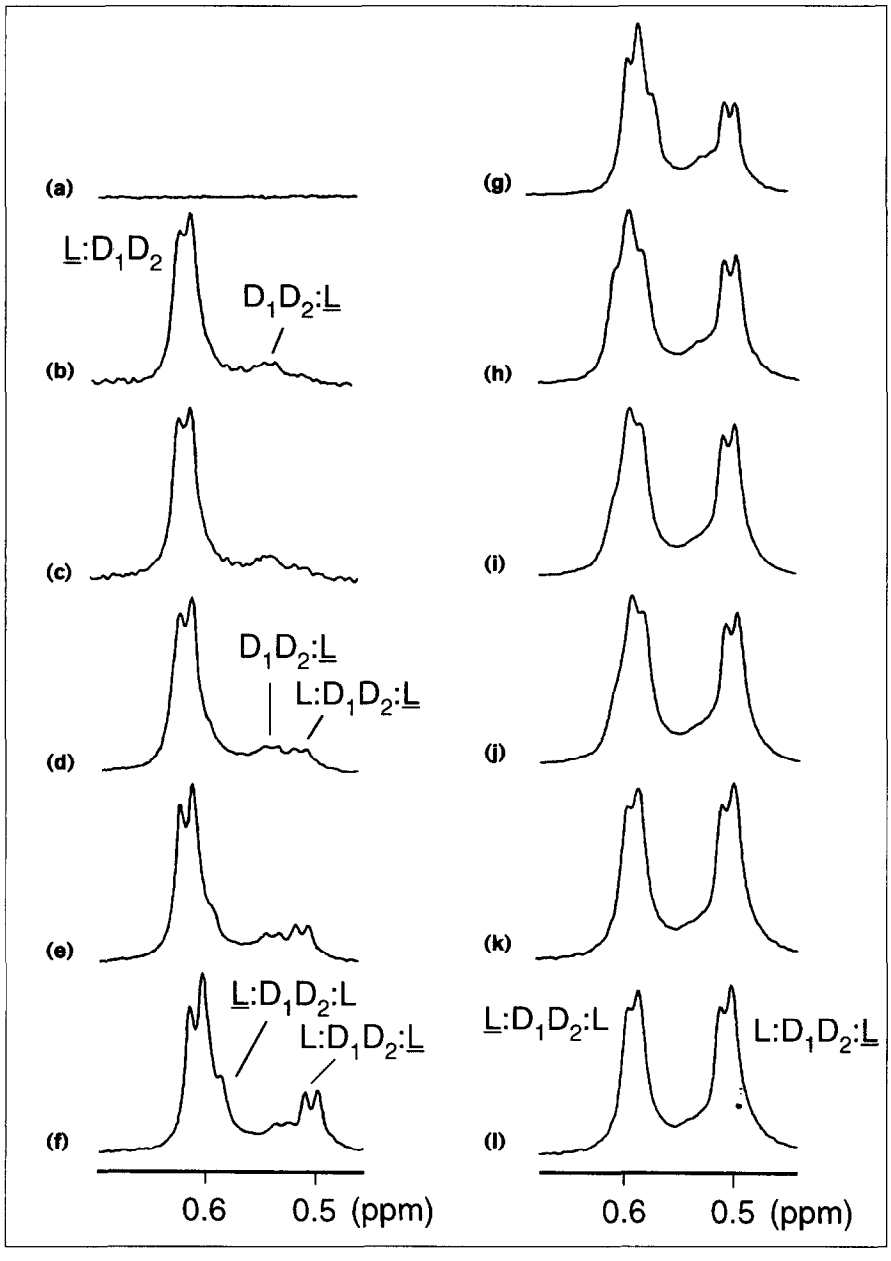

The D_1 site of the preformed dimer has higher affinity for ligand than the D_2 site. The spectra shown are 600 MHz ^{1}H NMR spectra (CD_3CN:D_2O, 1:4) at 283 K in the region of the carboxy-terminal D-Ala methyl resonance of di-*N*-ac-KDADA at various equivalence points in a ristocetin A solution (50 mM). **(a)** 0 equivalents of di-*N*-ac-KDADA, **(b)** 0.06, **(c)** 0.12, **(d)** 0.23, **(e)** 0.34, **(f)** 0.44, **(g)** 0.54, **(h)** 0.64, **(i)** 0.73, **(j)** 0.83, **(k)** 0.91, **(l)** 1.0 equivalent. D_1D_2 denotes the antibiotic dimer with two distinct binding sites (see text). LD_1D_2 denotes ligand bound to the D_1 site and D_1D_2L denotes ligand bound to the D_2 site. Underlining represents the bound ligand which gives rise to the resonance indicated.

di-*N*-ac-[d_8]-Lys-D-[d_3]-Ala-D-Ala (di-*N*-ac-[d_8]-KD-[d_3]-ADA) was titrated into a 3 mM solution of ristocetin A at 283 K. This analogue is a derivative of di-*N*-ac-KDADA, with a deuterated lysine side chain and a deuterated methyl group of the penultimate alanine, which function to remove the ligand signals that overlap with the Rh_6 methyl signals in the NMR spectra, such as the alanine methyl signals evident in Fig. 3b,c. In this titration it was possible to use both of the probes described above to observe ligand binding events to both sites in the dimer and to the monomer (Fig. 5). This titration shows that the preferred binding event involves ligand binding to the D_1 site of the dimer (1.33 ppm, Fig. 5b), followed by ligand binding to the monomer species (1.03 ppm, Fig. 5c), and then to the D_2 site of the dimer (0.93 ppm, Fig. 5d). In other words, the D_1 site of the dimer has the greatest affinity for the cell-wall analogue, and the monomer site has a greater affinity than the D_2 site of the dimer.

The dimerization constants at each stage of the titration were determined by integrating the Rh_6 methyl signals from the dimer (from the D_2 site) and monomer. These results are represented by the curve in Figure 6, which shows the variation of the dimerization constant with the amount of ligand present. Ligand binding to the D_1 site is cooperative with dimerization, raising the dimerization

constant from ~800 M^{-1} to ~1200 M^{-1}. The subsequent event of ligand binding into the D_2 site of the dimer reduces the amount of dimer present, shown by the decrease in the dimerization constant from ~1200 M^{-1} at the half way point of the titration to ~600 M^{-1} when the dimer is fully bound. This clearly demonstrates that binding of ligand into the less favored D_2 site leads to a reduction of the dimerization constant, and is thus responsible for the overall anti-cooperativity between ligand binding and dimerization for ristocetin A.

The free-energy diagram for ligand binding to ristocetin A

We have previously shown that an antibiotic dimer, in which both binding sites have the same affinity for ligand, can display a cooperative enhancement of dimerization with ligand binding, and we derived an energy diagram to describe this process [5]. Here, we have modified the free-energy diagram to describe the binding of di-*N*-ac-KDADA to the ristocetin A asymmetric dimer (with binding sites of different affinities) at 283 K (Fig. 7).

The free energy level **1** represents two molecules of monomeric ristocetin A, 2M, and two unbound molecules of the ligand di-*N*-ac-KDADA, 2L, in their ground-state conformations. The free energy difference **1→2** represents the formation of the asymmetric dimer, D_1D_2, from two molecules of monomer. The dimerization constant, $K_{1,2}$, for this process is 835 ± 150 M^{-1} ($\Delta G_{1,2}$ = −15.8 ± 0.5 kJ mol^{-1}).

Similarly, the energy difference **6→7** represents the formation of the asymmetric dimer bound to two molecules of ligand, formed from two molecules of monomeric ristocetin A, each bound to one molecule of ligand. This dimerization constant is calculated from the relative populations of the ligand-bound monomer and dimer species and is 585 ± 150 M^{-1} ($\Delta G_{6,7}$ = −15.0 ± 0.5 kJ mol^{-1}).

The ligand binding energies of the antibiotic have been measured using UV spectrophotometry. These studies were performed at sufficiently low concentration of

Figure 5

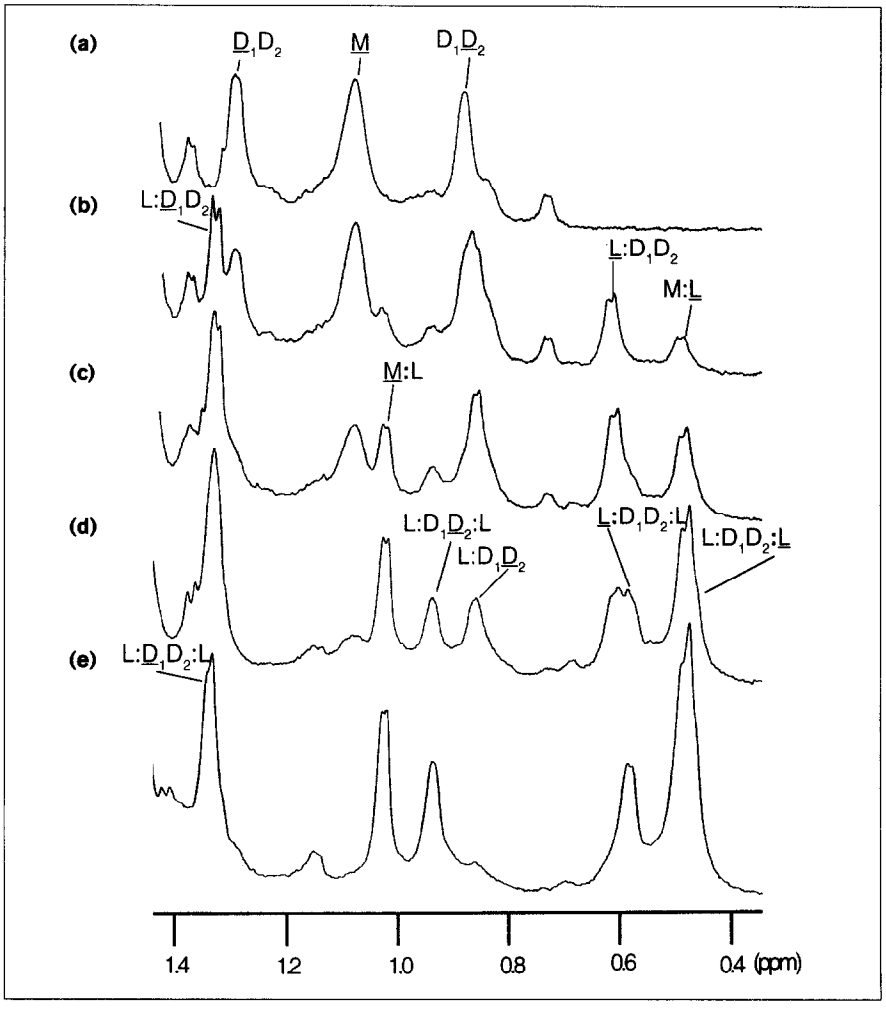

The D_1 site of the dimer has the greatest affinity for di-*N*-ac-KDADA, and the monomer site has a greater affinity than the D_2 site of the dimer. The spectra shown are 500 MHz ^1H NMR spectra (D_2O) at 283 K in the region of the ristocetin A Rh_6 and carboxy-terminal D-Ala methyl resonances in the titration of di-*N*-ac-[d_8]-KD-[d_3]-ADA into a 3 mM ristocetin A solution. **(a)** 0 equivalents of di-*N*-ac-[d_8]-KD-[d_3]-ADA, **(b)** 0.17, **(c)** 0.39, **(d)** 0.64, **(e)** 1.0 equivalent. M denotes antibiotic monomer and D_1D_2 denotes the antibiotic dimer with the two distinct binding sites (see text). LD_1D_2 denotes ligand bound to the D_1 site and D_1D_2L denotes ligand bound to the D_2 site. L represents the bound ligand which gives rise to the carboxy-terminal Ala methyl resonance indicated. M and D represent the antibiotic monomer or the monomeric partner within the dimer, respectively, that gives rise to the Rh_6 methyl resonance indicated.

Figure 6

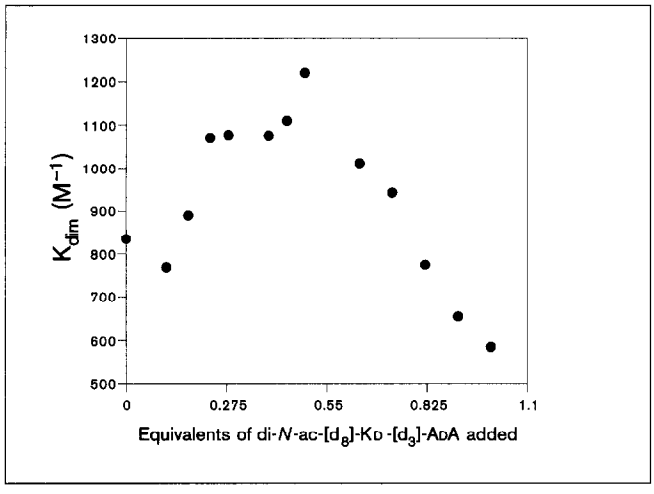

Ligand binding to the D_1 site is cooperative, whereas subsequent binding to the D_2 site is anti-cooperative. A plot of the change in binding constant (K_{dim}) between ristocetin A and di-*N*-ac-[d_8]-KD-[d_3]-ADA, as a function of added di-*N*-ac-[d_8]-KD-[d_3]-ADA is shown. Binding to the D_1 site raises K_{dim}; subsequent binding to the D_2 site reduces the amount of dimer present as indicated by the reduction in K_{dim}.

ristocetin A that it was essentially all monomer. The binding constant of monomeric ristocetin A with di-*N*-ac-KDADA, represented by the free energy difference **1→5** is $K_{1,5} = 8.6 \pm 1.9 \times 10^5\ M^{-1}$ ($\Delta G_{1,5} = -26.7 \pm 0.5$ kJ mol^{-1}). The ligand-binding energies of the D_1 and D_2 sites of the antibiotic, when the remaining site is free, were determined by measuring the relative populations of the ligand bound signals and the free antibiotic signals (see experimental section for more detail); these are $\Delta G_{2,3} = -23.0 \pm 1.0$ kJ mol^{-1} and $\Delta G_{2,4} = -27.9 \pm 1.0$ kJ mol^{-1}.

Where free energies could not be experimentally determined (for example the binding energies of di-*N*-ac-KDADA into the D1 or D2 sites of dimer with the other site already occupied) values were calculated from the free energy diagram. These free energies were calculated as $\Delta G_{3,7} = -29.6 \pm 1.4$ kJ mol-1 and $\Delta G_{4,7} = -24.7 \pm 1.4$ kJ mol^{-1}.

Consequences of the free-energy diagram

The energy diagram (Fig. 7) illustrates the cooperativity between dimerization and ligand binding to the D_1 site. This site has a greater ligand binding energy (~–27.9 kJ mol^{-1}) than the monomer (M) site (~–26.7 kJ mol^{-1}). Upon the subsequent filling of the D_2 site, however, dimerization becomes anti-cooperative, as this site has a lower ligand binding energy (~–24.7 kJ mol^{-1}) than the monomer site. This is illustrated clearly by the decrease in the dimer population upon the subsequent binding of ligand to the less favored site, D_2 (Fig. 6).

Significance

The role of dimeric structures in biological processes is widespread and well known (for example, [15–17]). The interdependence between dimerization and binding to another molecule (e.g., ligand or cofactor) is often important in physiological processes. Perhaps the most well known example of this interdependence is that displayed by hemoglobins, where the affinity for oxygen and the sigmoidal shape of the binding curve is dependent upon the strength of the dimer interaction of the protein, the pH, and the concentrations of diphosphoglycerate (DPG) and chloride ions [16]. The oxygen affinity of the related molecule myoglobin, which exists as a monomer, does not display the same dependence on the concentration of H^+, DPG or Cl^-

Figure 7

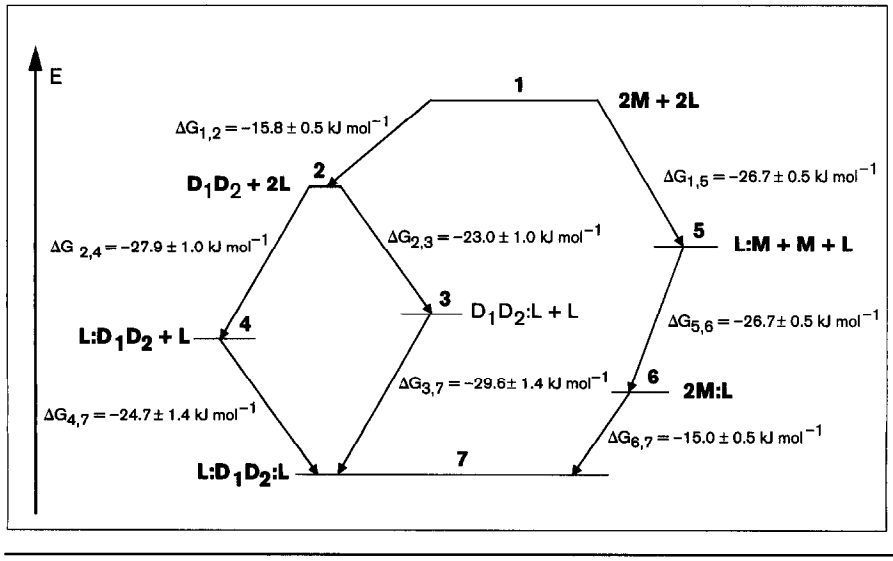

The free-energy diagram for di-*N*-ac-KDADA binding to ristocetin A. The left half of the energy diagram follows the process of dimerization and the subsequent binding of two ligand molecules. The right half of the diagram follows the process of ligand binding to monomer, followed by dimerization. The differences between the energy levels were determined as described in the text.

[17]. Thus, to gain any advantage from these factors, the oxygen carrier must exist as a dimer.

The dimeric structures of the vancomycin group of antibiotics studied to date (with the exception of the monomeric teicoplanin and the ristocetin A dimer considered here) have been shown to facilitate cooperativity between dimerization and the binding of the natural ligand [7]. In other words, ligand binding to antibiotic dimer is more favorable than to monomer and dimerization is more favorable when ligand is bound. This cooperativity is believed to enhance the activity of the antibiotic, particularly when an antibiotic dimer can bind simultaneously to two mucopeptide cell wall precursors that are attached to the same bacterial cell membrane [8].

Here, we have investigated the overall anti-cooperative nature of the asymmetric homodimer of ristocetin A, an antibiotic that has distinct binding affinities for ligand in each half of the dimer. We have shown that binding to one half of the dimer remains cooperative such that ligand binding to this dimer half is stronger than to antibiotic monomer. Ligand binding to the other half of the dimer, however, is less favorable than to the monomer such that when the less favorable binding site of the dimer is filled, the dimerization constant is reduced — an anti-cooperative effect. An asymmetric dimer with two distinct affinities for ligand may be a common mechanism for the fine tuning of activity or physiological response. For the bacterial aspartate receptor, which is a dimeric receptor, ligand induced asymmetry of the dimer modulates the affinity for aspartate [18]. Controlling the interdependence of dimerization and ligand binding in this way avoids the need to alter the residues which directly form the binding site. Changing these residues without causing drastic changes in activity may be very difficult, but more subtle control may be exerted if structural changes are made that indirectly affect dimerization and ligand binding [18].

Materials and methods

Materials

The antibiotic ristocetin A was kindly provided by Abbott Laboratories (Chicago) as the sulphate salt. D-Alanine, D-alanyl-D-alanine and di-*N*-acetyl-lysyl-D-alanyl-D-alanine were purchased from Sigma. D-[d_3]-Alanine and L-[d_8]-lysine were purchased from Eurisotope. Di-*tert*-butyldicarbonate was purchased from Aldrich and HBTU (2-(1H-benzotriazole-1-yl)-1,1,3,3-tetramethyluronium hexafluorophosphate) was purchased from Novabiochem.

One-dimensional ^{1}H NMR spectra were recorded on a Bruker DRX 500 MHz spectrometer and a Varian Unity Plus 600 MHz spectrometer using a standard pulse sequence. Spectra were recorded with 32 K data points and referenced with respect to either residual protio solvent (δ = 7.26 ppm for $CDCl_3$, δ = 2.52 ppm for d_6-DMSO) or internal 3-(trimethylsilyl)-1-propanesulphonate (TSP, δ = 0.00 ppm).

Ristocetin A was prepared for NMR titration studies by lyophilization twice from D_2O, followed by dissolution in a pD 7.0 buffer (KD_2PO_4 (0.1 M)/NaOD (0.1 M)). Ligand samples were similarly prepared but were finally taken up in the buffered ristocetin A solution (200 µl) to maintain the same antibiotic concentration during titrations. All titrations were performed using stepwise additions of the ligand solution (5 or 10 µl aliquots) into antibiotic solution. All pD sample readings were measured with a Corning 125 pH meter equipped with a combination glass electrode at 25 °C. The pD values quoted throughout are pH meter readings, and no corrections have been made for isotope effects.

The determination of the binding constant between ristocetin A and di-*N*-ac-KDADA was done using a UVIKON 940 dual beam spectrophotometer at 283 K. Ristocetin A (1.08 mg, 0.50 µmol) was taken up in aqueous buffer (0.1 M KH_2PO_4/NaOH, pH 7.0, 10 ml). Two ligand solutions (1.5 ml, 190 mM) were prepared, one from the antibiotic solution and the other from the buffer solution. The λ_{max} for ristocetin A was determined by measuring the UV spectrum with antibiotic solution in the sample beam and a buffer solution in the reference beam. The λ_{max} for the antibiotic–ligand complex was determined by measuring the UV spectrum after the addition of 1 ml of ligand/antibiotic solution to the sample cell, and 1 ml of ligand/buffer solution to the reference cell. The greatest differences in λ between the antibiotic and antibiotic–ligand complex fell in the region of 280–294 nm, and a smaller difference in the region of 240–250 nm. The titration was performed by adding aliquots of the ligand/antibiotic and ligand/buffer solutions to the sample and reference cell respectively, and measuring the absorbance at 244, 246, 280, and 284 nm after each addition of ligand. The data at 244 and 246 nm were added together and subtracted from the sum of the data at 280 and 284 nm. The resulting data set was plotted against the concentration of the ligand added, resulting in a smooth binding curve. This curve was analyzed using the proprietary non-linear curve-fitting routine of Abelbeck software's Kaleidagraph version 2.1.3.

Preparation of N-*acetyl-*D*-alanyl-*D*-alanine*

D-Alanyl-D-alanine (100 mg, 0.62 mmol) was dissolved in water (1 ml) and distilled acetic anhydride (1 ml) was added. The solution was stirred for 2 h at room temperature and the solvent was removed under reduced pressure to give an oil. Repeated lyophilization of the residue yielded *N*-acetyl-D-alanyl-D-alanine as a white powder (124 mg, 98 %) which was used without further purification.

Preparation of t-*Boc-*D*-[d_3]-alanine*

D-[d_3]-Alanine (300 mg, 3.30 mmol) and di-*t*-butyldicarbonate (840 mg, 3.80 mmol) were dissolved in a mixture of acetonitrile (1.5 ml) and sodium hydroxide solution (3 M, 4 ml). The solution was stirred for 3 h, after which time further sodium hydroxide solution (3 M, 1 ml) was added so as to maintain the pH above 9.5. Stirring was continued overnight and the reaction mixture was then washed with ether (2 x 20 ml). The aqueous layer was then acidified with hydrochloric acid solution (3 M) to pH 1 and was extracted with ethyl acetate (3 x 20 ml). The combined ethyl acetate extracts were washed with brine (30 ml), dried over anhydrous sodium sulfate and filtered. The filtrate was evaporated to dryness under vacuum to yield *t*-Boc-D-[d_3]-alanine (552 mg, 88 %) as an off-white waxy solid which was used without further purification.

Preparation of t-*Boc-*D*-alanine benzyl ester*

t-Boc D-alanine (8.0 g, 42 mmol) was dissolved in ethyl acetate (140 ml) to which benzyl bromide (12.2 g, 71 mmol) and triethylamine (7.7 g, 76 mmol) were added. The resulting mixture was heated at reflux for 18 h. The mixture was then filtered and the residue was washed with ethyl acetate (2 x 30 ml). The combined filtrates were then washed with hydrochloric acid solution (1 M, 2 x 80 ml), water (80 ml), sodium hydrogen carbonate solution (10 % w/v, 2 x 80 ml) and brine (80 ml). The organic layer was then dried over anhydrous sodium sulfate, filtered and evaporated to dryness to afford *t*-Boc-D-alanine benzyl ester (8.3 g, 71 %) as a colorless oil, which was used without further purification.

Preparation of t-*Boc-*D*-[d_3]-alanyl-*D*-alanine benzyl ester*
t-Boc-D-alanine benzyl ester (780 mg, 2.80 mmol) was dissolved in a mixture of dichloromethane (4 ml) and a solution of anhydrous hydrogen chloride in dioxane (4 M, 4 ml) and stirred for 2 h. The solvent was then removed to afford crude D-alanine benzyl ester hydrochloride as a white solid. The crude material was then dissolved in dichloromethane (4 ml) and *N,N*-diisopropylethylamine (400 mg, 3.09 mmol) and added to a mixture of *t*-Boc-D-[d_3]-alanine (540 mg, 2.80 mmol), *N,N*-diisopropylethylamine (410 mg, 3.17 mmol) and HBTU (1.25 g, 3.30 mmol) in dichloromethane (6 ml), which had previously been stirred for 10 min. The resulting solution was stirred at room temperature for 30 min and then washed with hydrochloric acid solution (3 M, 3 x 20 ml), sodium hydrogen carbonate solution (10 % w/v, 2 x 20 ml), brine (30 ml), dried over anhydrous sodium sulfate, filtered and evaporated to dryness. The residue obtained was then chromatographed over silica (chloroform) to afford *t*-Boc-D-[d_3]-alanyl-D-alanine benzyl ester (790 mg, 80 %) as a white waxy solid. ^{1}H NMR (500 MHz; CDCl3; 300 K) δ 1.40 (3 H, d, *J* 7.2 Hz), 1.43 (9 H, s), 4.12–4.17 (1 H, m), 4.61 (1 H, app quin), 4.97–5.02 (1 H, m), 5.16 (2 H, ABq, J_{AB} 7.8 Hz), 6.60–6.70 (1 H, m), 7.31–7.38 (5 H, m).

*Preparation of di-*t*-Boc-*L*-[d_8]-lysine*
L-[d_8]-Lysine monohydrochloride (40 mg, 0.21 mmol) and di-*t*-butyldicarbonate (110 mg, 0.50 mmol) were dissolved in a mixture of acetonitrile (250 ml) and sodium hydroxide solution (3 M, 350 ml) and the pH of the solution was adjusted to greater than 9 by the addition of further sodium hydroxide solution (3 M, 350 ml). The mixture was stirred overnight and then washed with ether (2 x 10 ml) and the aqueous layer was acidified to pH 1 by the addition of hydrochloric acid solution (3 M), which resulted in a milky solution. The acidified aqueous layer was then extracted with ethyl acetate (3 x 10 ml) and the combined extracts were dried over anhydrous sodium sulfate, filtered and evaporated to dryness to afford crude di-*t*-Boc-L-[d_8]-lysine as a pale brown glassy solid (68 mg, 91 %) which was used without further purification.

*Preparation of di-*t*-Boc-[d_8]-lysyl-D-[d_3]-alanyl-D-alanine benzyl ester*
t-Boc-D-[d_3]-alanyl-D-alanine benzyl ester (65 mg, 0.18 mmol) was dissolved in a mixture of dichloromethane (1 ml) and a solution of anhydrous hydrogen chloride in dioxane (4 M, 1 ml) and stirred for 2 h. The solvent was then removed to afford crude D-[d_3]-alanyl-D-alanine benzyl ester hydrochloride as a white solid. This residue was then taken up in a mixture of dichloromethane (1 ml) and *N,N*-diisopropylethylamine (a sufficient amount to solubilize the hydrochloride salt) and added to a solution of di-*t*-Boc-[d_8]-lysine (68 mg, 0.19 mmol), HBTU (95 mg, 0.25 mmol) and *N,N*-diisopropylethylamine (100 mg, 0.77 mmol) in dichloromethane (1 ml), which had previously been stirred for 10 min. The resulting solution was stirred for 2 h and then washed with hydrochloric acid solution (3 M, 2 x 20 ml), sodium hydrogen carbonate solution (10 % w/v, 2 x 20 ml), brine (30 ml), dried over anhydrous sodium sulfate, filtered and evaporated to dryness. The residue obtained was then chromatographed over silica (methanol:chloroform, 5:95) to afford di-*t*-Boc-[d_8]-lysyl-D-[d_3]-alanyl-D-alanine benzyl ester (77 mg, 73 %) as a white crystalline solid. ^{1}H NMR (500 MHz; $CDCl_3$) δ 1.36–1.45 (21 H, m), 3.97–4.05 (1 H, m), 4.50 (1 H, d, *J* 7.5 Hz), 4.56 (1 H, app quin), 4.65 (1 H, bs), 5.15 (2 H, ABq, J_{AB} 13.5 Hz), 5.30 (1 H, bs), 6.84–6.86 (1 H, m), 6.97–6.99 (1 H, m), 7.30–7.36 (5 H, m).

*Preparation of di-*N*-acetyl-[d_8]-lysyl-D-[d_3]-alanyl-D-alanine benzyl ester*
Di-*t*-Boc-[d_8]-lysyl-D-[d_3]-alanyl-D-alanine benzyl ester (77 mg, 0.13 mmol) was dissolved in dichloromethane (2 ml) and a solution of anhydrous hydrogen chloride in dioxane (4 M, 2 ml) and stirred for 90 min. The solvent was then removed to afford crude L-[d_8]-lysyl-D-[d_3]-alanyl-D-alanine benzyl ester dihydrochloride. This was then suspended in a mixture of dichloromethane (5 ml) and *N,N*-diisopropylethylamine (750 mg, 5.80 mmol) and acetic anhydride (200 mg, 1.96 mmol) and stirred for 3 h. The mixture was then evaporated to dryness and chromatographed over silica (methanol:chloroform 1:4). The major band was collected and evaporated to dryness to afford di-*N*-acetyl-[d_8]-lysyl-D-[d_3]-alanyl-D-alanine benzyl ester as a white solid (45 mg, 73 %). ^{1}H NMR (500 MHz; d_6-DMSO) δ 1.30 (3 H, d, *J* 7.3 Hz), 1.75 (3 H, s), 1.80 (3 H, s), 4.14 (1 H, d, *J* 7.5 Hz), 4.25–4.32 (2 H, m), 5.09 (2 H, ABq, 13.0 Hz), 7.30–7.39 (5 H, m), 7.71 (1 H, bs), 7.96 (1 H, d, *J* 7.5 Hz), 8.11 (1 H, d, *J* 7.9 Hz), 8.23 (1 H, d, *J* 7.0 Hz).

*Preparation of di-*N*-acetyl-[d_8]-lysyl-D-[d_3]-alanyl-D-alanine*
Di-*N*-acetyl-[d_8]-lysyl-D-[d_3]-alanyl-D-alanine benzyl ester (45 mg, 0.09 mmol) was dissolved in absolute ethanol (10 ml) and Pd/C (5 %, 5 mg) was added and the reaction mixture was hydrogenated at 1 atm for 12 h. The mixture was then flushed with nitrogen, filtered through celite and evaporated to dryness. The solid obtained was then lyophilized from deionized water to afford di-*N*-acetyl-[d_8]-lysyl-D-[d_3]-alanyl-D-alanine as a white solid (35 mg, 96 %). ^{1}H NMR (500 MHz; 60 % D_2O/H_2O) δ 1.31 (3 H, d, *J* 7.2 Hz), 1.88 (3 H, s), 1.94 (3 H, s), 4.11–4.15 (1 H, m), 4.16–4.22 (1 H, m), 4.23–4.26 (1 H, m), 7.82 (1 H, bs), 8.04 (1 H, d, *J* 6.5 Hz), 8.12 (1 H, d, *J* 6.5 Hz), 8.27 (1 H, d, *J* 6.5 Hz).

Determination of the dimerization constant of ristocetin A
The dimerization constants for ristocetin A when free ($K_{1,2}$) and bound to di-*N*-ac-KDADA ($K_{6,7}$) were determined by measuring the relative integrals of the Rh_6 methyl NMR signals for monomer and dimer species obtained at different concentrations of antibiotic at 283 K. The relative integrals were determined by cutting and weighing the signals from the plotted spectra. The concentration of dimer was plotted against the total concentration of antibiotic, and the resulting curve was analyzed using the proprietary non-linear curve fitting routine of Abelbeck Software's Kaleidagraph version 2.1.3.

Determination of the binding constant for the D_1 site
The binding constant of di-*N*-ac-KDADA to the D_1 site of the ristocetin A dimer, with the D_2 site free, was determined using the following equation:

$$K_{2,4} = \frac{[LD_1D_2]}{[D_1D_2][L]}$$

The concentrations were determined from NMR data from a solution obtained by adding 0.06 equivalents of di-*N*-ac-KDADA to a 50 mM ristocetin A solution. The total dimer population was measured by determining the average integral of the D_1 and D_2 signals and this total weight was taken to be equivalent to 25 mM.

[L] is the free ligand concentration, and under these conditions this concentration is difficult to measure since most of the ligand is bound to the antibiotic. Since the total ligand concentration was known (the amount of ligand added, 3 mM), and the two ligand-bound dimer species are measurable from the NMR spectra, [L] could be determined using the following relationships:

$$[D_{total}] = [D_1D_2] + [LD_1D_2] + [D_1D_2L]$$

$$[L_{total}] = [L] + [LD_1D_2] + [D_1D_2L]$$

Once this binding constant (ligand binding into D_1 with D_2 free) was determined, the binding constant for ligand into the D_2 site with D_1 free was attainable, as the free energy difference between LD_1D_2 and D_1D_2L was known ($\Delta G_{3,4} = -4.9 \pm 0.5$ kJ mol^{-1}).

Acknowledgements

We are grateful to the Biomedical NMR Center, National Institute for Medical Research, Mill Hill, London, for the use of NMR facilities and to Abbott Laboratories (Chicago) for the gift of ristocetin A. Thanks for financial support to Smithkline Beecham (A.J.M, Y.R.C), Overseas Research Students Awards Scheme (Y.R.C.), Cambridge Commonwealth Trust (Y.R.C), C.T. Taylor Fund (Y.R.C), Xenova (A.C.T, P.G.), EPSRC (M.S.W., P.G.), and Glaxo Research and Development Ltd. (M.S.W.).

References

1. Barna, J.C.J. & Williams, D.H. (1984). The structure and mode of action of glycopeptide antibiotics of the vancomycin group. *Annu. Rev. Microbiol.* **38**, 339–357.
2. Nagarajan, R. (1993). Structure–activity relationships of vancomycin-type glycopeptide antibiotics. *J. Antibiot. (Tokyo)* **46**, 1181–1195.
3. Nieto, M. & Perkins, H.R. (1971). The specificity of combination between ristocetins and peptides related to bacterial cell wall mucopeptide precursors. *Biochem. J.* **124**, 845–852.
4. Williams, D.H., Williamson, M.P., Butcher, D.W. & Hammond, S.J. (1983). Detailed binding sites of the antibiotics vancomycin and ristocetin A: determination of intermolecular distances in antibiotic/substrate complexes by use of the time-dependent NOE. *J. Am. Chem. Soc.* **105**, 1332–1339.
5. Groves, P., Searle, M.S., Waltho, J.P. & Williams, D.H. (1995). Asymmetry in the structure of glycopeptide antibiotic dimers: NMR studies of the ristocetin A complex with a bacterial cell wall analogue. *J. Am. Chem. Soc.* **117**, 7958–7964.
6. Mackay, J.P., Gerhard, U., Beauregard, D.A., Maplestone, R.A. & Williams, D.H. (1994). Dissection of the contributions toward dimerisation of glycopeptide antibiotics. *J. Am. Chem. Soc.* **116**, 4573–4580.
7. Mackay, J.P., Gerhard, U., Beauregard, D.A., Westwell, M.S., Searle, M.S. & Williams, D.H. (1994). Glycopeptide antibiotic activity and the possible role of dimerization: a model for biological signalling. *J. Am. Chem. Soc.* **116**, 4581–4590.
8. Beauregard, D.A., Williams, D.H., Gwynn, M.N. & Knowles, D.J.C. (1995). Dimerization and membrane anchors in extracellular targeting of vancomycin group antibiotics. *Antimicrob. Agents Chemother.* **39**, 781–785.
9. Groves, P., Searle, M.S., Mackay, J.P. & Williams, D.H. (1994). The structure of an asymmetric dimer relevant to the mode of action of the glycopeptide antibiotics. *Structure* **2**, 747–754.
10. Prowse, W.G., Kline, A.D., Skelton, M.A. & Loncharich, R.J. (1995). Conformation of A82846B, a glycopeptide antibiotic, complexed with its cell wall fragment: an asymmetric homodimer determined using NMR spectroscopy. *Biochemistry* **34**, 9632–9644.
11. Sheldrick, G.M., Paulus, P., Vertesy, L. & Hahn, F. (1995). Structure of ureido-balhimycin. *Acta Crystallogr. B* **51**, 89–98.
12. Batta, G., Cristofaro, M.F., Sharman, G.J. & Williams, D.H. (1996). Demonstration of the difference in binding affinity between the two binding sites of the ristocetin A asymmetric dimer. *J. Chem. Soc., Chem. Commun.* **1**, 101–103.
13. Groves, P., Searle, M.S., Chicarelli-Robinson, I. & Williams, D.H. (1994). Recognition of the cell-wall binding site of the vancomycin group antibiotics by unnatural structural motifs: ^{1}H NMR studies of the effects of ligand binding on antibiotic dimerisation. *J. Chem. Soc. [I],* 659–665.
14. Groves, P., Searle, M.S., Westwell, M.S. & Williams, D.H. (1994). Expression of electrostatic binding cooperativity in the recognition of cell-wall peptide analogues by vancomycin group antibiotics. *J. Chem. Soc., Chem. Commun.* 1519–1520.
15. Ullrich, A. & Schlessinger, J. (1990). Signal transduction by receptors with tyrosine kinase activity. *Cell* **61**, 203–212.
16. Ackers, G.K. & Halverson, R. (1974). The linkage between oxygenation and subunit dissociation in human hemoglobin. *Proc. Nat. Acad. Sci. USA* **71**, 4312–4316.
17. Perutz, M.F. (1978). Hemoglobin structure and respiratory transport. *Sci Am* **239**, 92–125.
18. Biemann, H.-P. & Koshland Jr, D.E. (1994). Aspartate receptors of *Escherichia coli* and *Salmonella typhimurium* bind ligand with negative and half-of-the-sites cooperativity. *Biochemistry* **33**, 629–634.